Fractal Analyses of High-Resolution Cloud Droplet Measurements

SZYMON P. MALINOWSKI* AND MONIQUE Y. LECLERC

Department of Physics, University of Quebec at Montreal, Montreal, Quebec, Canada

DARREL G. BAUMGARDNER

National Center for Atmospheric Research, Boulder, Colorado

(Manuscript received 20 July 1992, in final form 23 June 1993)

ABSTRACT

Fractal analyses of individual cloud droplet distributions using aircraft measurements along one-dimensional horizontal cross sections through clouds are performed. Box counting and cluster analyses are used to determine spatial scales of inhomogeneity of cloud droplet spacing. These analyses reveal that droplet spatial distributions do not exhibit a fractal behavior. A high variability in local droplet concentration in cloud volumes undergoing mixing was found. In these regions, thin filaments of cloudy air with droplet concentrations close to those observed in cloud cores were found. Results suggest that these filaments may be anisotropic. Additional box counting analyses performed for various classes of cloud droplet diameters indicate that large and small droplets are similarly distributed, except for the larger characteristic spacing of large droplets.

A cloud–clear air interface defined by a certain threshold of total droplet count (TDC) was investigated. There are indications that this interface is a convoluted surface of a fractal nature, at least in actively developing cumuliform clouds. In contrast, TDC in the cloud interior does not have fractal or multifractal properties. Finally a random Cantor set (RCS) was introduced as a model of a fractal process with an ill-defined internal scale. A uniform measure associated with the RCS after several generations was introduced to simulate the TDC records. Comparison of the model with real TDC records indicates similar properties of both types of data series.

1. Introduction

The concept that clouds may be described as fractals was introduced by Mandelbrot (1982) and Lovejoy (1982). Fractal and multifractal properties of radar and satellite images of clouds have been investigated by Cahalan and Joseph (1989) and Lovejoy and Schertzer (1990). The influence of the multifractal structure of clouds on radiative processes has recently been considered by Davis et al. (1991). In spite of those works, cloud descriptions in terms of fractal geometry and multifractal measures have so far received little attention in the cloud physics community, reflecting partly that fractal studies of clouds have been few and very recent. In contrast, in the turbulence research field, the fractal approach has brought new ideas in the understanding of the energy cascade and the intermittence of turbulent energy (Mandelbrot 1974; Meneveau and Sreenivasan 1991), and in the description of turbulent entrainment and mixing (Sreenivasan et al. 1989). Recently, Malinowski and Zawadzki (1993, hereafter referred to as MZ) adopted the Sreenivasan et al. (1989) approach to entrainment and mixing in turbulent flows to clouds, obtaining realistic times of cloud dissipation. They investigated fractal properties of one-dimensional (1D) horizontal sections through fields of continental fair weather cumuli and found that on such a cross section, points delineating clear air from cloudy filaments form a fractal set of dimension $D_1 = 0.55$.

Observations allowing an analysis of cloud droplet distribution at scales below 1 mm are scarce. Holographic measurements of very small cloud and fog volumes have been analyzed (e.g., Conway et al. 1982; Kozikowska et al. 1984). Baumgardner (1986) developed a method for measuring interarrival times of droplets detected by the Particle Measuring System's (Boulder, CO) Forward Scattering Spectrometer Probe (FSSP). Such data was used by Paluch and Baumgardner (1989) to investigate the Baker et al. (1984) hypothesis of inhomogeneous mixing in clouds from fluctuations of droplet concentrations. They found that in mixed cloud regions, a high degree of nonuniformity in droplet concentration on a scale of meters exists. They also noticed that the production of large droplets due to supersaturation during ascent of diluted volumes is unlikely. Finally, they argued that the mixing process

* On leave from the University of Warsaw, Poland.

Corresponding author address: Szymon P. Malinowski, University of Warsaw, Institute of Geophysics, o2-093 Warszawa ul. Pasteura 7, Poland.

is not an instantaneous one capable of influencing cloud dynamics. These findings are consistent with those of Brenguier (1990). Based on the analysis of the coincidence effect of the droplet sampler, he argued that regions with low average droplet concentrations are in fact heterogeneous, containing volumes of local droplet concentrations as high as those in cloud cores. Recently Baker (1992a) used a new statistical test (the "fishing test") on the measured interarrival times of droplets to investigate their spatial distribution on segments 100 m long. He found that inhomogeneities in droplet concentration are often observed in regions seemingly homogeneous at large scales. These findings all lead to the conclusion that the small-scale structure of cloud volumes undergoing mixing is an important feature, which should be further investigated.

In this paper the authors use fractal techniques to investigate small-scale features of Hawaiian rainband clouds. Interarrival times of individual cloud droplets are analyzed to infer fractal properties of droplet distributions along a penetration approximately 40 km long through the rainband. The recorded interarrival times are then degraded to obtain TDC (total droplet count) on segments of various lengths. Multifractal properties of these TDC series are investigated. Fractal properties of the cloud–clear air interface are investigated in a manner described in MZ. The TDC record is thresholded, and points at the threshold value define cloud filament–clear air interface. This approach does not distinguish between nature of cloud or clear air filaments. "Cloud filaments" can be understood here as

- filaments formed during entrainment–mixing process,
- separate towers,
- separate clouds,
- cloud interiors.

Finally, TDC from HARP and from continental fair weather cumuli are compared to the simple, artificially generated, fractal—the random Cantor set (hereafter RCS). The RCS was chosen, according to the suggestion of MZ, to be irregular in contrast to standard Cantor sets. RCS may prove useful in the understanding of turbulent entrainment and mixing. In particular, if a realistic model of a two-stage process of stretching and convolution of cloud–clear air interface by turbulence followed by molecular and sedimental mixing across a thin layer (Sreenivasan et al. 1989; MZ) is adopted, RCS may correspond to the one-dimensional section through a volume after a first stage of such a process.

2. The experimental data

The data used in this paper were collected during flight 20 of HARP. Observations were made at a constant altitude of 1790 m (816 mb). Cloud bases were approximately 600 m AGL (940 mb). Six consecutive clouds were penetrated during a straight line pass along the rainband over a distance of approximately 40 km. Temperatures at cloud base and flight level were about 19°C and 12°C, respectively. Aircraft speed was 110 m s^{-1}. The FSSP Droplet Spacing Monitor (DSM), described in detail by Baumgardner et al. (1993), has a maximum theoretical temporal resolution of 1 μs, which provides a measure of distances between individual cloud droplets with a 0.11-mm spatial resolution. The real resolution was, however, smaller due to dead time loss of the sensor and could be estimated as 8 μs (0.9 mm). Droplets with diameters ranging from 2 to 48 μm were detected and grouped in 15 classes.

The FSSP continuously sweeps a small area perpendicular to the flight direction. This has the advantage that measurements can be treated as a 1D horizontal section though clouds. The recorded interarrival times of droplets can be interpreted as a set of points of known positions along a segment. Subsets of droplets of various diameters can also be investigated. Data on interarrival times can be degraded to give TDC on segments of various lengths. TDC on segments 1 m long collected during the entire flight leg is presented in Fig. 1. Six separate clouds can be distinguished from this data: cloud 1 covering the first 3000 m of the record, cloud 2 from 6.5 to 8.5 km, dissipating cloud 3 (12 to 14 km), cloud 4 (17–23 km), cloud 5 (23–25 km), and cloud 6 (25–39 km). Since the last cloud consists of segments of visibly different TDC, an additional segment (35–39 km) of cloud 6 was investigated. An analysis of the flight video reveals that clouds were in various stages of development, with younger clouds prevailing in the first part of the flight and older, more stratiform clouds in the second part. Figure 2 illustrates the droplet spacing distribution as a function of distance. While peaks observed around 1 mm and 1 m are representative of the device resolution and cloud physics processes (see next paragraphs), the peak at 10 cm is an artifact and any physical interpretation of the behavior of the distribution in that region should be witheld: a detailed investigation of the dataset indicated that this peak is due to an occasional resetting of the DSM electronics leading to a spurious insertion of an interarrival time of 1024 μs into the data stream. The dataset was processed with all 1024-μs interarrival times removed to investigate the effect of this error on subsequent analyses. Careful tests were conducted on the set and showed that fractal results are independent of this artifact.

An example of measurements of TDC on segments of various lengths in two different clouds (2 and 3) is presented in Fig. 3. As with the 1-m resolution (Fig. 3a), individual cumuliform cloud can easily be identified in the left-hand side of the plot, and the interface between cloud and clear air filaments is well delineated.

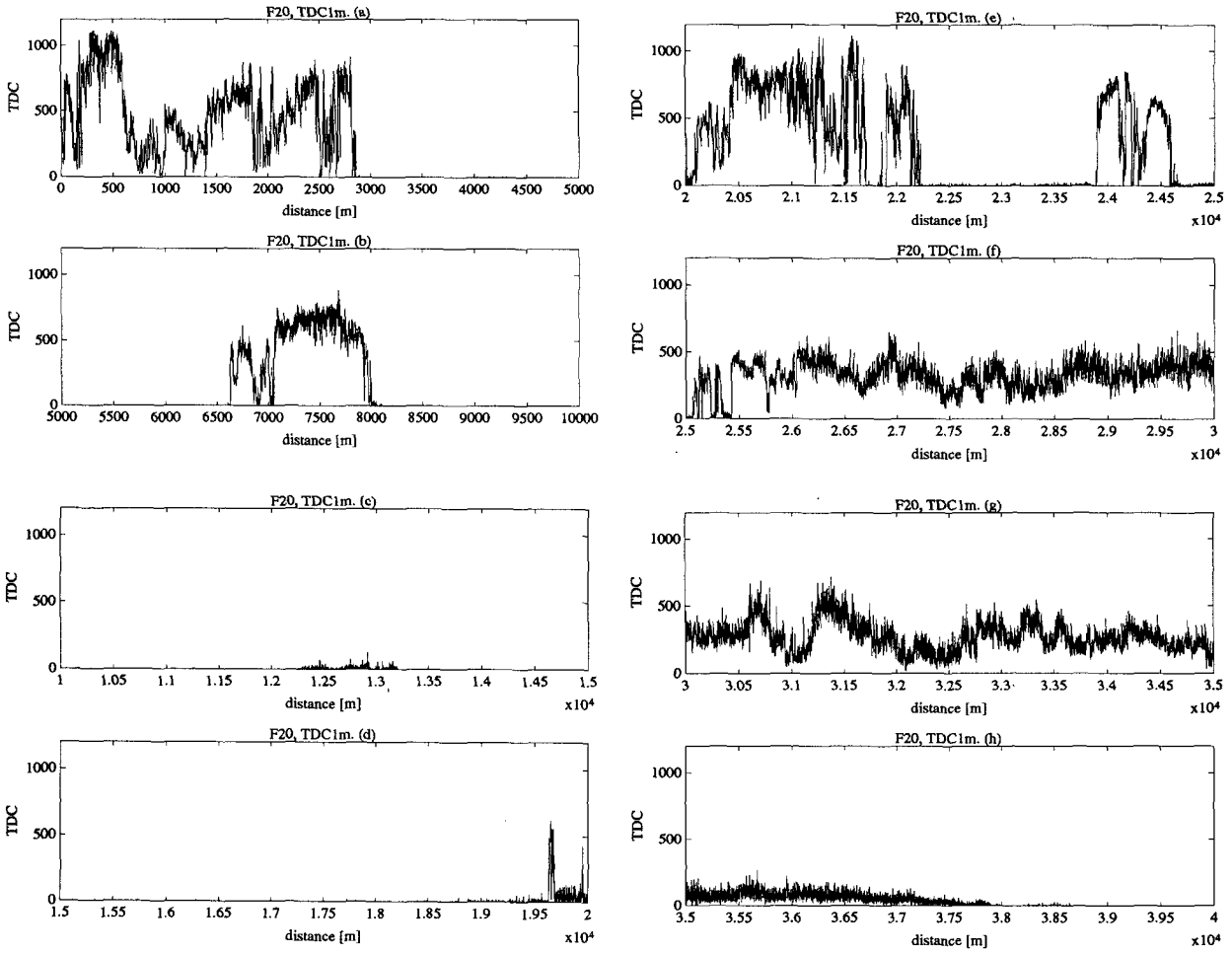

FIG. 1. Total droplet count (TDC) on 1-m segments: the entire flight.

The presence of cloud remnants is apparent on the right-hand side of the graph. In contrast, the 1-cm resolution picture is different since the level of fluctuations is comparable to the maximum TDC. The interface between cloudy and clear air filaments cannot be easily identified. An explanation of this property can be attributed to the FSSP configuration. The strobe count comes from particles passing through the laser beam of 0.2 mm in diameter and 12 mm long. A parallelepiped with area 2.4 mm^2 sweeps through the cloud during the flight. The binomial sampling theorem indicates that more than 100 droplets must be counted before statistical fluctuations would be expected below 10% of that value. Thus, for typical concentrations of 400 cm^{-3} found in Hawaiian clouds, an average pathlength of approximately 10 cm is necessary to maintain statistical fluctuations below 10% of the mean value. In this case, only scales much larger than the probe's theoretical resolution can be investigated. Thus, TDC on 11-cm segments was analyzed in order to investigate geometrical properties of the cloud–clear air interface.

3. Data analysis

Cloud droplets form a set of points in space. The interarrival times of individual droplets recorded by FSSP give one-dimensional (linear) section through such a set, resulting in a set of points on a straight line. Fractal properties of such a set can easily be investigated by means of box counting and cluster analysis. In brief, box counting is a technique to estimate the fractal dimension of a set. The space occupied by the set is divided into a number of boxes of some size r. If the number of boxes containing elements of the set N follows a power law as a function of box size

$$N(r) \sim r^{-D}, \tag{1}$$

then D is an estimate of the fractal dimension of the set [for details consult, e.g., Falconer (1990)]. Cluster analysis is another technique of estimating fractal dimension of a set (see Feder 1988). In this technique the number M of set elements inside a circle of diameter r centered on a given set element is counted and averaged over all set (all center points). If this average

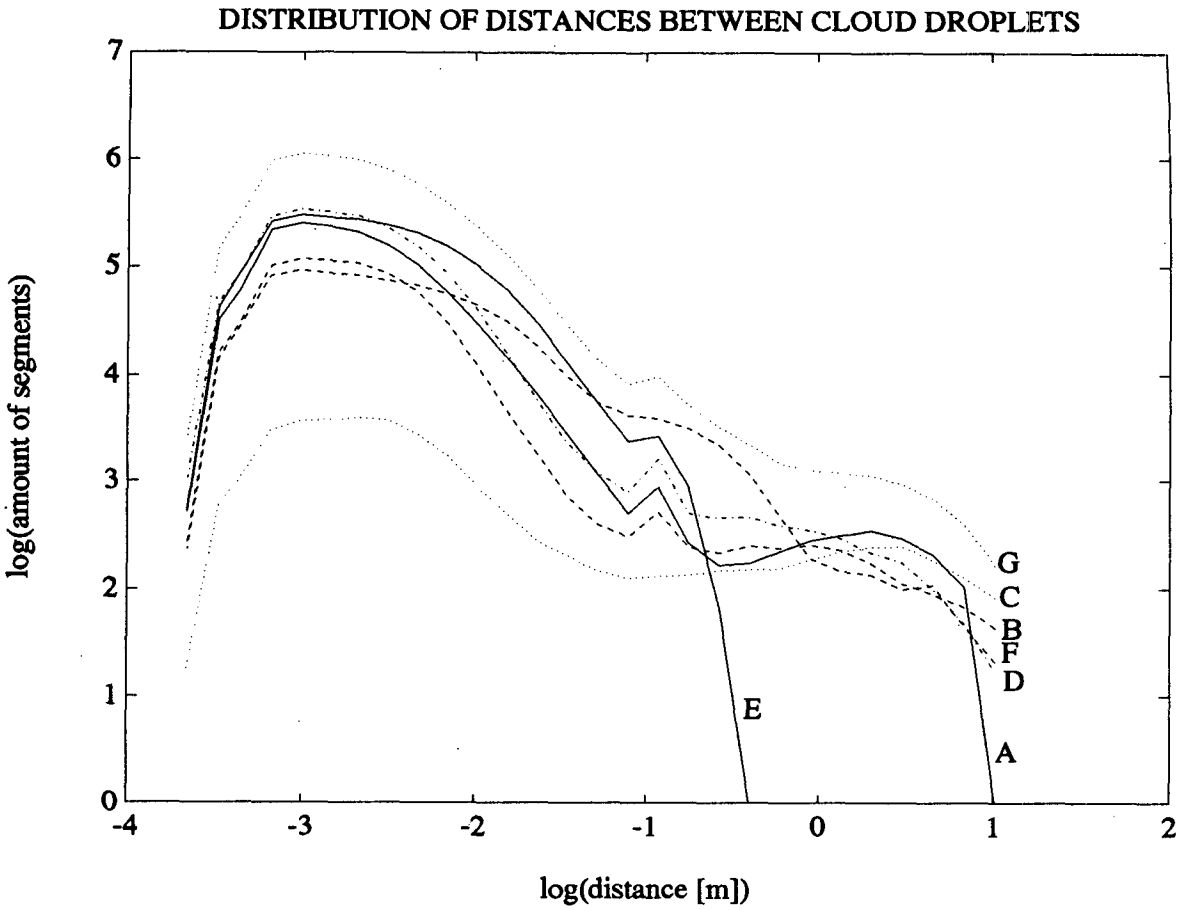

FIG. 2. Distribution of distances between cloud droplets: (a)–(f) for successive segments of lengths of 6.6 km; (g) for the whole flight.

$\langle M \rangle$ follows a power law as a function of a circle diameter r,

$$\langle M \rangle(r) \sim r^D, \tag{2}$$

the power law exponent is another estimate of the fractal dimension. The range of box sizes resulting in power laws is called scaling range. Conveniently, scaling ranges appear as linear regions on log–log plots, and exponents of power laws (scaling exponents) are determined from the slope of these linear regions. The internal and integral scales are determined by left and right ends of linear regions on log–log plots, respectively. Breaking and lack of the scaling properties are indicated by inflexion points or curvatures, respectively.

Two segments of data were investigated using cluster analysis (Fig. 4) and results agreed with those using the box counting technique. Figure 5 presents results of box counting for seven segments and for the entire set. All segments exhibit a similar behavior at small (0.1–1 mm) and large (1 m–1 km) scales. At large scales, the slopes of all lines are close to -1 (exact values are in range -0.93 to -0.99) indicating "space filling" in terms of fractal dimension (a slope of -1 corresponds to the fractal dimension $D_1 = 1$). At small scales, the slope approaches 0, which is in agreement with the fact that data are recorded with better resolution than FSSP can give. Curves start to bend from horizontal ones at scales slightly below 1 mm, which corresponds to the FSSP resolution. At scales of 1 cm–1 m, the behavior of curves corresponding to clouds 1 and 2 is similar to that at large scales (slope about -0.96). The curve representing cloud 3 cannot be reasonably approximated at the intermediate scales (1 mm–1 m) by a straight line. In addition, curves corresponding to all clouds, clouds 4, 5, and segment 7 of cloud 6 taper off from slope close to -1 at the same range of scales 1 mm–1 m. Using the 1-m resolution TDC, cloud 2 (Fig. 1b) seems to be an active convective cloud in the developing stage, while cloud 3 (Fig. 1c) seems to be nearly dissipated. We can deduce that all other clouds consist of undissipated and dissipating volumes by comparing (Fig. 5) curve 6, corresponding to the whole cloud, with curve 7 corresponding to the

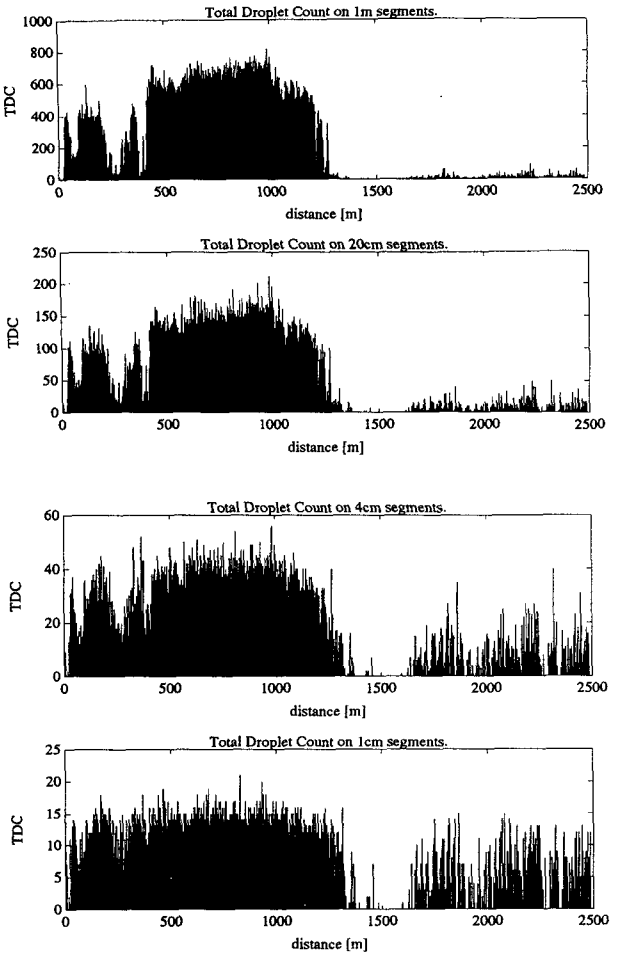

FIG. 3. TDC from high-resolution FSSP from clouds 2 and 3 (a 2-km region with no cloud droplets recorded has been omitted) collected on 1-m, 20-cm, 4-cm, and 1-cm segments from top to bottom, respectively.

most dissipated part of this cloud (Fig. 1h). However, the box counting technique weighs subsets of higher fractal dimension more than those of lower dimension. Thus, the effect of undissipated volumes usually prevails over dissipating ones, and curves 4, 5, 6, and 7 correspond more to curves 1 and 2 than to curve 3. Similar box counting was performed on selected classes of droplet diameters with the goal of determining whether or not large droplets have a tendency to be grouped in clusters. Results are presented in Fig. 6. It can be seen that the region with slope 0 for the large droplets is larger than that for the small ones and covers scales resolved by FSSP. This means that the characteristic distance between large droplets is longer than that for the small droplets. At large scales, the slope for large droplets approaches 1; that is, it is the same as for small droplets, with no tendency for multiscale clustering (no portion of the curve with slope different from 0 or 1). The transition region between slope 0 and 1 is smooth and spans about two orders of magnitude, regardless of the droplet radius range and with exception of cloud 3 (dissipating one).

An interesting property of the entrainment–mixing process can be observed by analyzing TDC data at a 2.2-cm resolution (5000 Hz). Examples of such plots from cloud interiors, volumes close to the cloud edge that undergo intensive mixing as well as dissipating clouds, are given in Fig. 7. The presence of thin (several centimeters) sheets or strings of cloudy air with larger filaments of clear air in between is clearly indicated. Similar findings are reported by Baker (1992b). A comparison of TDC in these sheets with TDC observed inside the cloud interior suggests that local droplet concentrations often reach a maximum equal to concentrations in the cloud cores, supporting findings of Paluch and Baumgardner (1989) on the convoluted nature of cloud–clear air interface. This is also in agreement with results of Brenguier (1990) and strongly supports the recent approach to cloud microphysics parameterization developed by Brenguier and Grabowski (1993).

As mentioned, the TDC collected on segments 11 cm long was analyzed in order to investigate fractal properties of the cloud–clear air interface. The TDC record was thresholded and box counting was applied to the points at the threshold value. Calculations for a span of thresholds from 1 to maximum TDC observed were made and results for the whole dataset as well as for individual clouds are presented in Fig. 8. In most plots (clouds 1–5), two regions can be distinguished: one with the smaller slope at the small scales (hereafter referred as A) and the second with the steeper slope at larger scales (hereafter referred as B). The transition between these two regions varies from cloud to cloud and is generally shifted to small scales with increasing threshold. For thresholds of 2 (droplets counted on 11-cm segment) and more, slopes in the A region range from -0.44 to -0.62 corresponding to values reported by MZ. Slopes in the B region, for cloud 6 and for the whole dataset, range from -0.65 to -0.95. This differs significantly from the MZ findings, where the slope was constant over the entire range of investigated scales and was threshold independent.

TDC, being a positive defined function, is a measure. The figures presented above clearly show that TDC in some regions is highly intermittent. Such intermittent measures can often be described in terms of multifractals. In order to describe multifractal properties of a measure, a sequence of moment exponents $\tau(q)$ and multifractal spectrum should be retrieved. To do so the measure (TDC) should be integrated (coarse grained) on boxes of some size r, then raised to qth power (moment order q) and averaged over a set. In analogy with box counting, if such averaged moments $\langle M_q \rangle$ follow power laws with exponents $\tau(q)$ as functions of box size

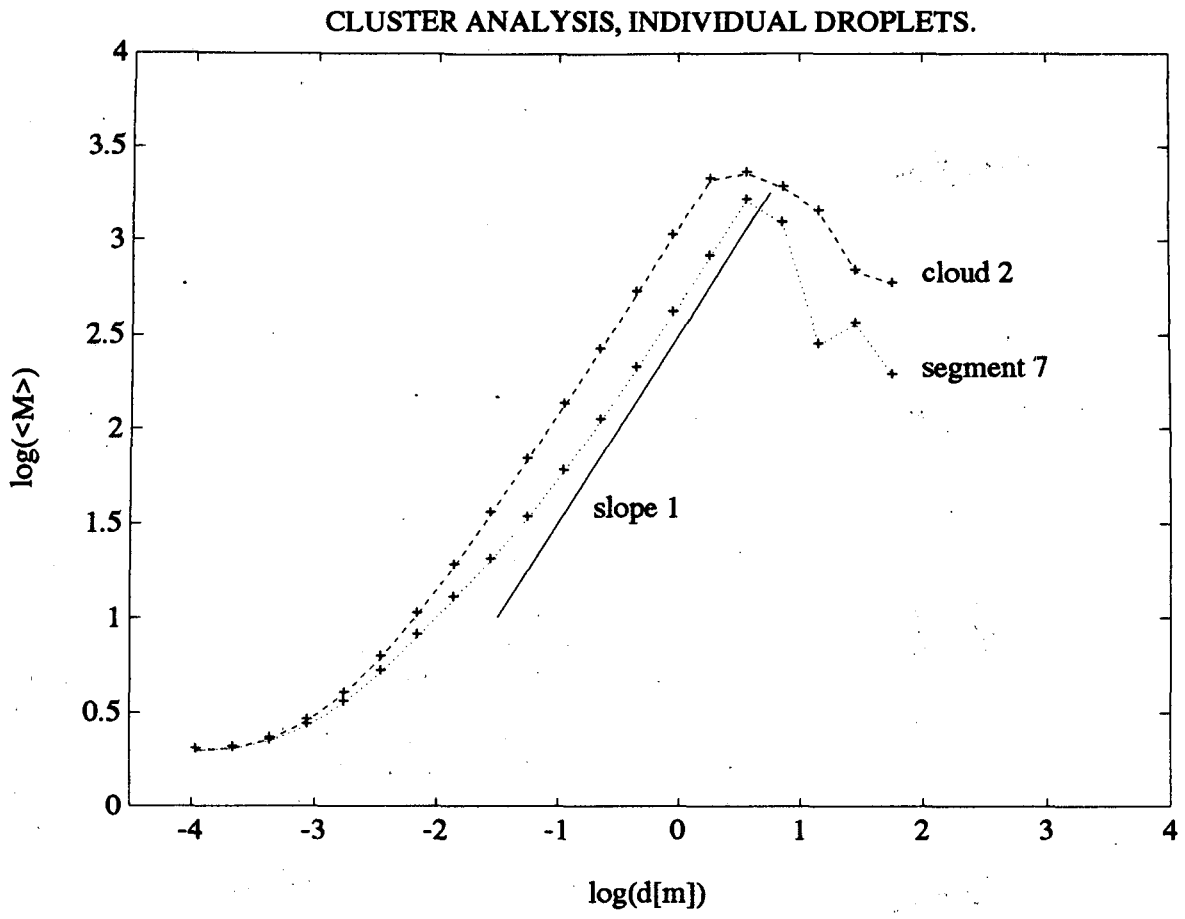

FIG. 4. Results of cluster analysis of positions of individual droplets. Cloud 2 (solid line) and segment 7 (dashed line).

$$\langle M_q \rangle \sim r^{\tau(q)}, \tag{4}$$

the measure is multifractal. Its singularity spectrum $f(\alpha)$ can be defined by a Legendre transform of $\tau(q)$:

$$\alpha = \partial\tau/\partial q; \quad f(\alpha) = q\alpha - \tau. \tag{5}$$

Readers are referred to the work of Mandelbrot (1989) or Feder (1988) for a comprehensive description of the latter.

An analysis of TDC moments in the range of scales from 1.1 cm to tens of kilometers is given in Fig. 9. Positive moments scale well in scales from 1.1 cm to kilometers. Scaling of negative moments, in contrast, is questionable even at smallest scales. The reason is a small amount of samples with weak singularities, which are magnified by negative moments. The $\tau(q)$ (slope vs moment order) retrieved for positive moments in a range of scales 2.2 cm–500 m is a straight line with a slope of 0.96, indicating a monofractal behavior with fractal dimension $f = \text{const} = D_1 = 0.96$ (multifractal behavior should result in a convex curve). Thus, f can be interpreted as a fractal dimension of the TDC support, that is, the set in which droplets are distributed. The slope $D_1 = 0.96$ obtained here corresponds very well to the value of fractal dimension as estimated by box counting on positions of individual droplets. Since all practical methods of estimating fractal dimension underestimate its value, results confirm "space filling" ($D_1 = 1$) droplet distribution.

Results of moment analysis performed on data investigated by MZ (TDC in continental fair weather cumuli recorded with 1-m resolution) are presented in Fig. 10. These are consistent with those of Hawaiian rainband clouds, indicating a monofractal behavior with $f = D = 0.97$. A scaling break suggesting a different behavior at small scales is clearer here than in the Hawaiian rainband cloud data (where only the leftmost points corresponding to the scale of 1.1 cm are deflected from a straight line on Fig. 9a). Unfortunately, the range of scales with this different behavior is too small to estimate multifractal properties in this range.

4. The model

To simulate the sequence of cloudy and clear air filaments penetrated, an artificial dataset was con-

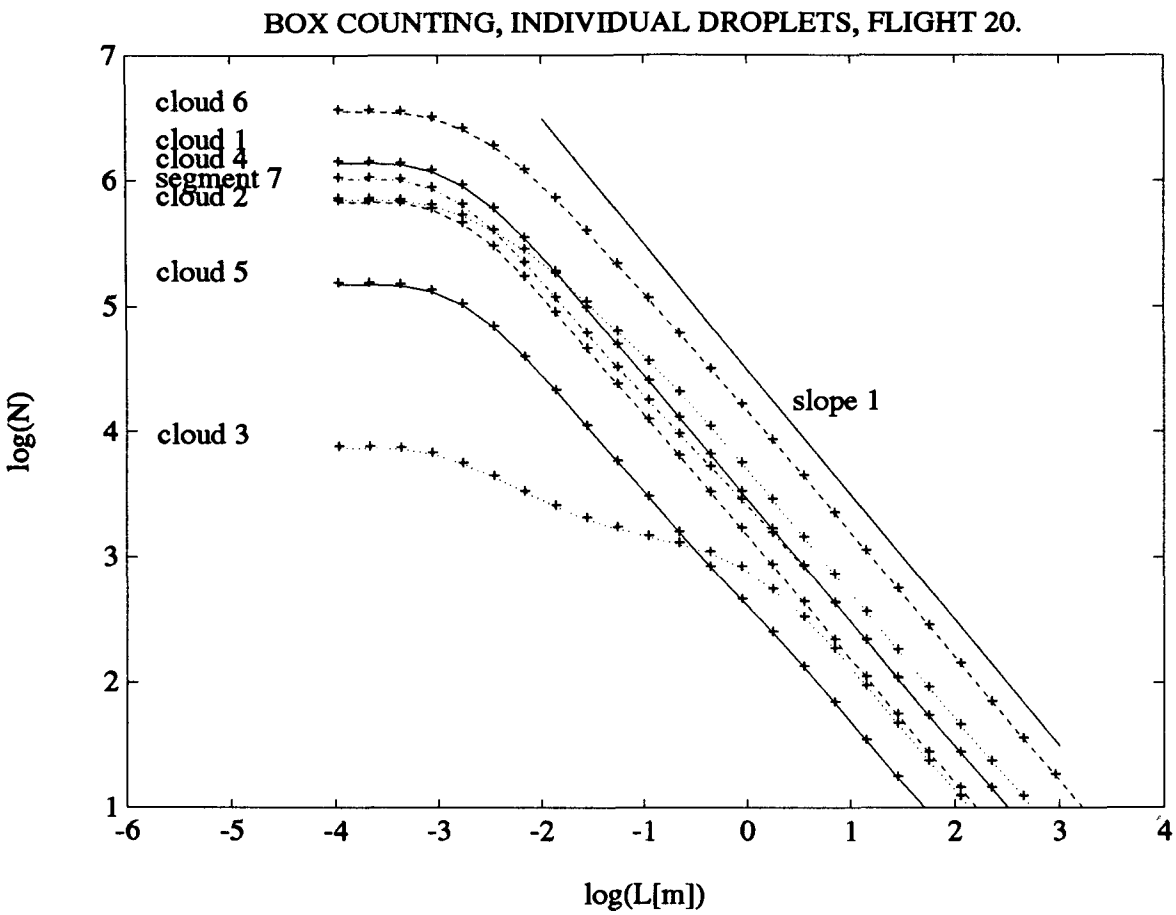

FIG. 5. Box counting analysis on individual droplets. All droplets detected by FSSP probe (diameters 2–47 mm) accounted for. L: box size, N: amount of boxes occupied by at least one droplet. Results for the whole dataset as well as for individual clouds.

structed. Up to 21 iterations of both a triadic (hereafter TCS) and a random (hereafter RCS) Cantor set (Falconer 1990) were performed. It was also assumed that segments remaining after these operations correspond to penetrations through cloud filaments. The RCS used here was obtained by removing, in successive iterations, randomly positioned segments of one-third length remaining after the previous iteration. The random number generator giving uniform distribution on segment [0, 1] was adopted as a source of randomness in the model. A uniform measure superimposed on RCS after nine iterations is shown in Fig. 11. An example of box counting applied to uniform measure on TCS and RCS thresholded in a similar manner as TDC in order to obtain points analogous to cloud–clear air interface is shown in Fig. 12. Since the measure is uniform (with constant value equal 1), results are threshold independent. It can be seen that the fractal dimension of the RCS is independent of the random number generator seed but is smaller than for the corresponding TCS. This is also a property of two-scale Cantor sets (e.g., Feder 1988). Conclusions from the absence of linearity at the larger scales cannot be drawn because of the poor statistical sample on large boxes. The value of the fractal dimension of RCS $D_1 = 0.55$ corresponds well to findings of MZ in fair weather cumuli.

One of the properties distinguishing the RCS from the TCS is that the inner scale l (the length of segments remaining after n generations) is variable, depending on the number of iterations and on the particular realization. This is an important property of this model resembling the behavior of many natural systems. In particular, one-dimensional horizontal sections through cloud fields contain cloud segments of various lengths. A uniform measure, representing droplet concentration in the cloud interior, was then applied to the RCS. When droplet concentration is assumed to be conserved during mixing—as is the case in the first stage of mixing, when turbulence acts toward convolutions and filamentation of cloud volumes (e.g., Paluch and Baumgardner 1989; Jensen and Baker 1989)—fragmentation of successive iterations (generations) of the RCS should correspond to filamenta-

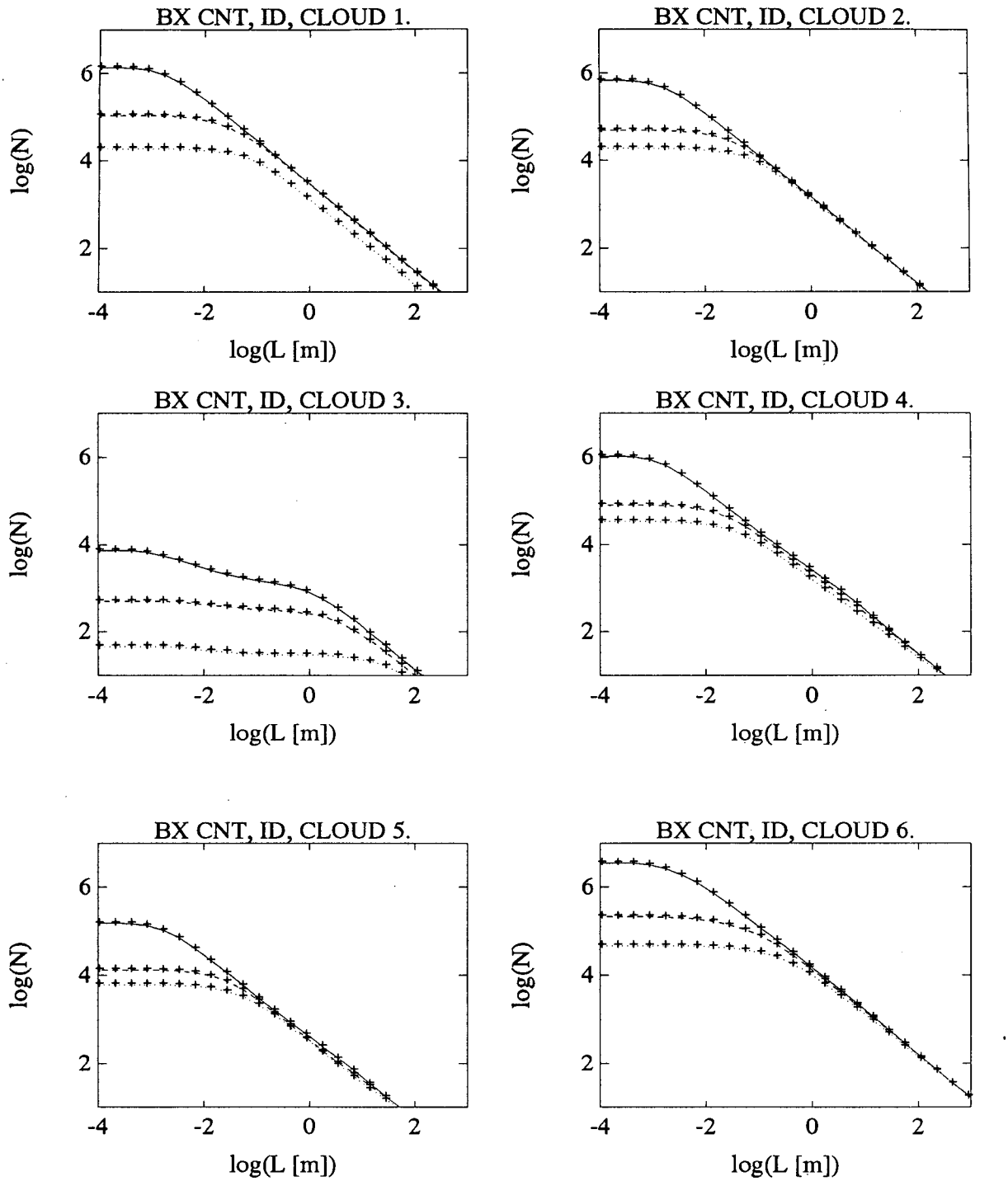

FIG. 6. Box counting analysis on individual droplets. Results for separate clouds. Solid line: all droplets, dashed line: droplets of diameters 17–47 μm, and dotted line: droplets of diameters 32–47 μm.

tion of cloud volumes due to turbulent mixing with a droplet-free exterior.

An analysis of moments of uniform measure on RCS after 9 and 18 iterations was performed and results compared with those of moment analysis on TDC records (Figs. 13, 14). When investigating positive moments (of order 0.5–5.5), it can be seen that for RCS the scaling is broken and two scaling ranges are present. The position of the breaking point between those two ranges depends upon a particular realization. The in-

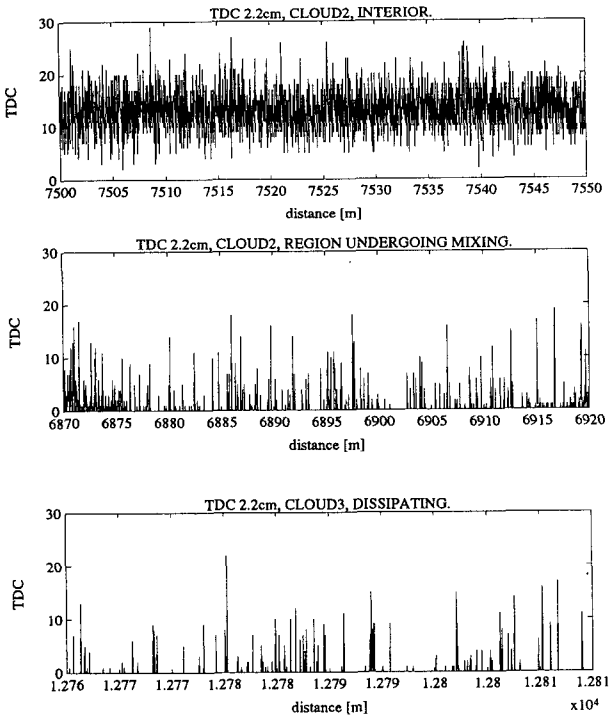

FIG. 7. Selected examples of TDC on 200-μs (2.2 cm) segments. Distance corresponds to Fig. 1.

flection point moves to smaller scales with increasing RCS generation levels [for 9 times iterated RCS is at log(segment size) ≈ -3.5; for 18 times iterated RCS is at log(segment size) ≈ -5.5]. This is because in the RCS an internal scale l is not well established: where l is larger than the segment size r, the local density of the measure can be defined and the integral of the measure on the box S has a different meaning than where $l < r$ and the definition of the measure density is not possible. Thus, scaling properties of positive moments are broken by the maximum observed internal scale l. The negative moments do not scale, similarly to TDC. The reason is that regions of weak singularities, emphasized by negative moments, are not present in the investigated series by the construction (uniform measure on the RCS). Now we retrieve, for positive moments only, the $\tau(q)$ function for two scaling ranges. At small scales, $\tau(q)$ is retrieved from the 11 smallest segment sizes of the 9 times iterated RCS. It clearly presents a linear behavior with slope 0.97. At large scales, $\tau(q)$ retrieved from the 17 largest segment sizes of 18 times iterated RCS exhibits a nearly linear behavior with slope 0.5. Estimating spectrum $f(\alpha)$ we obtain the monofractal behavior with single values of fractal dimension $f = D_1 = 0.97$ and $f = D_1 = 0.5$, for two scaling ranges, respectively. Results in the first scaling range (for 9 times iterated RCS) correspond well to the TDC properties. The second scaling range (or 18 times iterated RCS) corresponds to the very small scales resolving a fine structure of RCS. It is worth noting that this second estimate in the range where there is no influence of the internal scale gives smaller values of D_1 than the box counting estimate (Fig. 10) from which we get $D_1 = 0.55$. This may be attributed to slow convergence of $f(\alpha)$ with coarse graining to the final value (Mandelbrot 1989), or the slight curvature of $\tau(q)$ curve indicating weak multifractal properties of the model.

5. Discussion

Individual droplets in unmixed cloud volumes seem to fill the space in terms of fractal dimension at scales above 1 cm (Figs. 4 and 5). This implies that droplets are distributed randomly or regularly when investigating those volumes at scales above 1 cm. When entrainment and mixing develop, clear air filaments appear to cause departures from box counting curves on log–log plots from a slope of 1 (Fig. 5) and to create a secondary maximum or an extended tail of the distribution of distances between droplets (Fig. 2). The departure from slope 1 at the intermediate scales can be a rough indicator of the dissipation stage of the cloud. The absence of linear regions (on log–log plots) exhibiting a constant slope other than 0 or 1 suggests that droplet populations do not form fractal sets in regions undergoing dissipation. When investigating results of box counting for various sizes of droplets (Fig. 6), no tendency for clustering is observed. In fact, large droplets seem to be distributed in the same way as small ones, except for the larger characteristic distance between them. This may indicate that large droplets responsible for warm rain development in Hawaiian clouds are distributed randomly or uniformly in space at scales above 1 cm. This is consistent with findings of Paluch and Baumgardner (1989) in continental cumulus clouds that superadiabatic growth of precipitation droplets in diluted volumes is unlikely.

Results presented in Fig. 7 show that in volumes undergoing mixing, a high small-scale variability is expected and cloud fragmentation at those scales cannot be neglected. The data indicate that turbulence leads to the production of well-defined filaments observed even in nearly dissipated clouds. Thus, evaporative cooling is a local process occurring in a thin sheet on the cloud–clear air interface and it is incorrect to approximate it as uniform in a large volume. These sheets should be characterized by increased saturation (result of evaporation) leading to a persistence of cloudy filaments, particularly in regions of weak turbulence (inefficient stretching and thinning of sheets and filaments). The above may have an important influence in the analysis of low-resolution temperature and humidity observations. If these fields also exhibit a fine structure, estimates of total water content, virtual potential temperature, or entrainment levels obtained for cloud regions undergoing mixing are questionable (Malinowski and Pawlowska-Mankiewicz 1989).

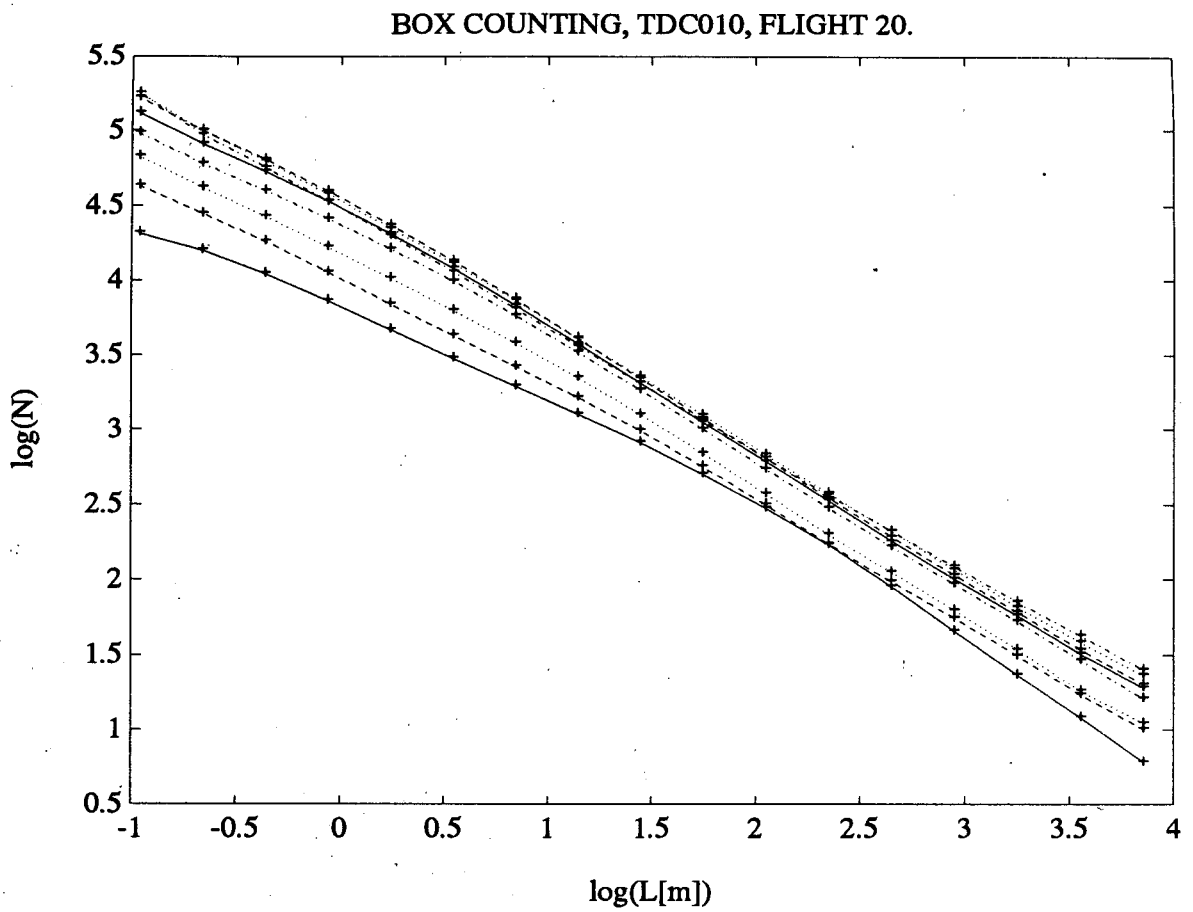

FIG. 8. Box counting on thresholded records of TDC on 11-cm segments. Results for thresholds of 1, 2, 4, 8, . . . droplets on the 11-cm segment from bottom to top, respectively. First plot for the whole flight, next plots for successive clouds.

The validity of the above findings is limited by the geometry of the investigated data. From 1D sections through clouds, conclusions concerning the 3D structure of a cloud droplet field have been deduced. For isotropic fractals this is not a limitation (Mandelbrot 1982), and temporal scales of the entrainment–mixing process can be estimated (MZ). This is, however, not the case in clouds and even small cloud filaments, where vertical anisotropy due to buoyancy and gravitational sedimentation of droplets exists. It is often argued that even in buoyant fluids, small-scale turbulence is isotropic due to the action of pressure forces. This, however, does not take into account droplet sedimentation, which is anisotropic regardless of the velocity fluctuations redistribution by pressure fluctuations. Due to anisotropy, sedimentation of cloud droplets leads to higher evaporation rates of horizontal filaments (where droplets fall across the underlying cloud–clear air interface into dry air) than vertical ones (where droplets fall along the saturated cloudy filament). This may lead to the longer lifetime of vertical filaments in regions of weak turbulence present in nearly dissipated clouds.

Results of the analysis of moments on both uniform measure on RCS after a moderate number of iterations and TDC indicate the similarity between these two series. Here $D_1 = 0.96$ obtained for TDC agrees well with results for individual droplets, is very close to unity, and suggests that cloud filaments are "space filling," that is, do not have fractal properties. The situation, however, looks different for the cloud–clear air interface, defined by a certain TDC threshold. Malinowski and Zawadzki (1993) reported that one-dimensional sections through such an interface have a fractal dimension $D_1 = 0.55$ over a wide range of thresholds. Figure 8 depicts similar power laws for most clouds at small scales and small thresholds. The breaking point for the scaling moves toward smaller scales with increasing threshold. The slope at the right-hand side of the breaking point increases with scale and threshold. This can be attributed to the difference of properties between Hawaiian rainband clouds and continental cumuli. Videotapes from the rainband flight indicate that both developing cumuliform clouds and more mature, stratiform clouds were encountered. The typical maxima of TDC on 11-cm segments for cumuli-

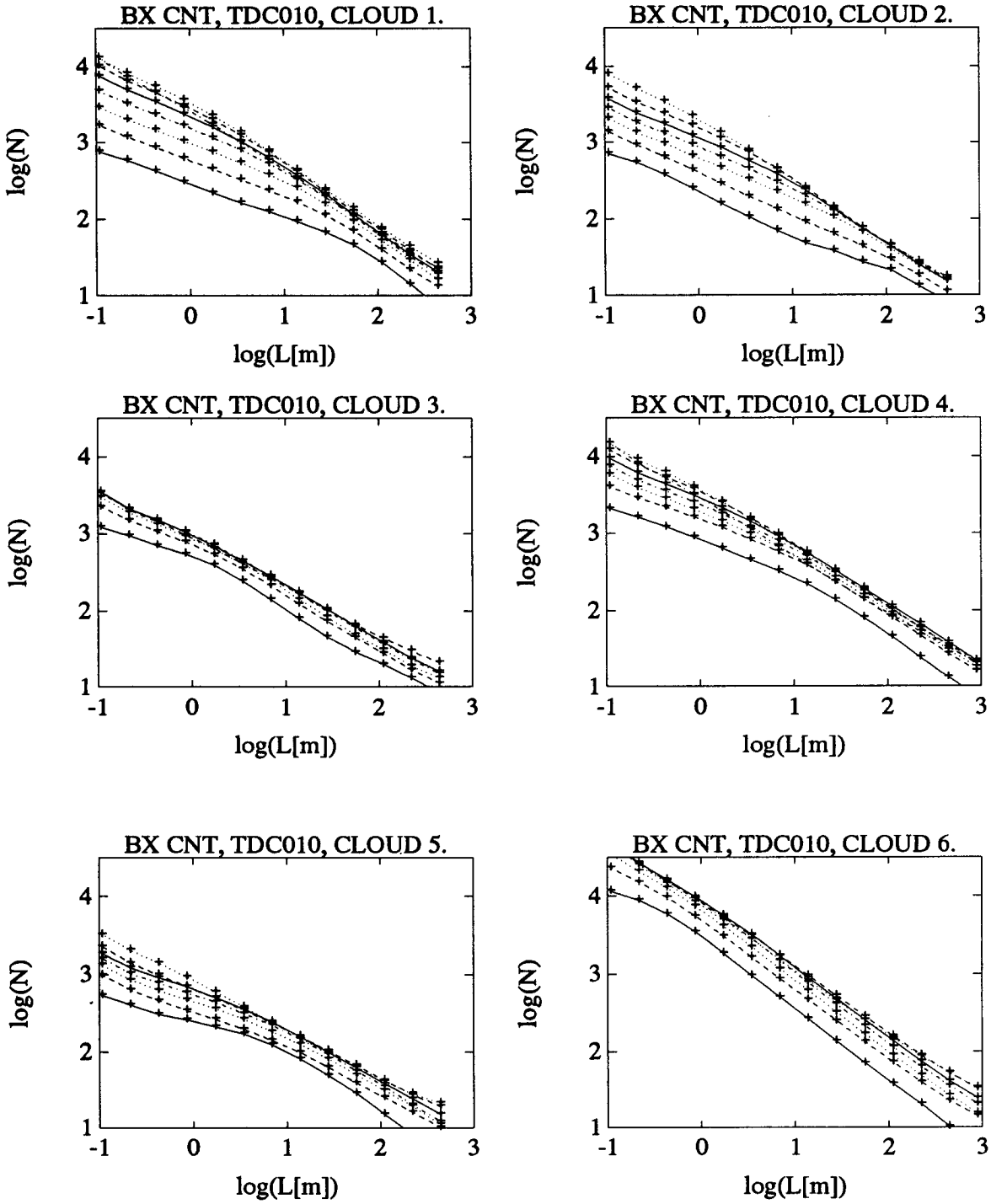

FIG. 8. (*Continued*)

form and stratiform clouds were about 140 and 70 counts, respectively, indicating the different character of these cloud volumes. Furthermore, Fig. 3 indicates a large variability of TDC on such segments due to the small FSSP volume. Thus, thresholding such data to perform functional box counting results in a set of points of various physical origin: either corresponding to "true" cloud–clear air interfaces or resulting from statistical fluctuations of TDC around different mean values in clouds in various stages of their life cycle. With increasing thresholds and box sizes, probability of hitting points of various physical origin increases,

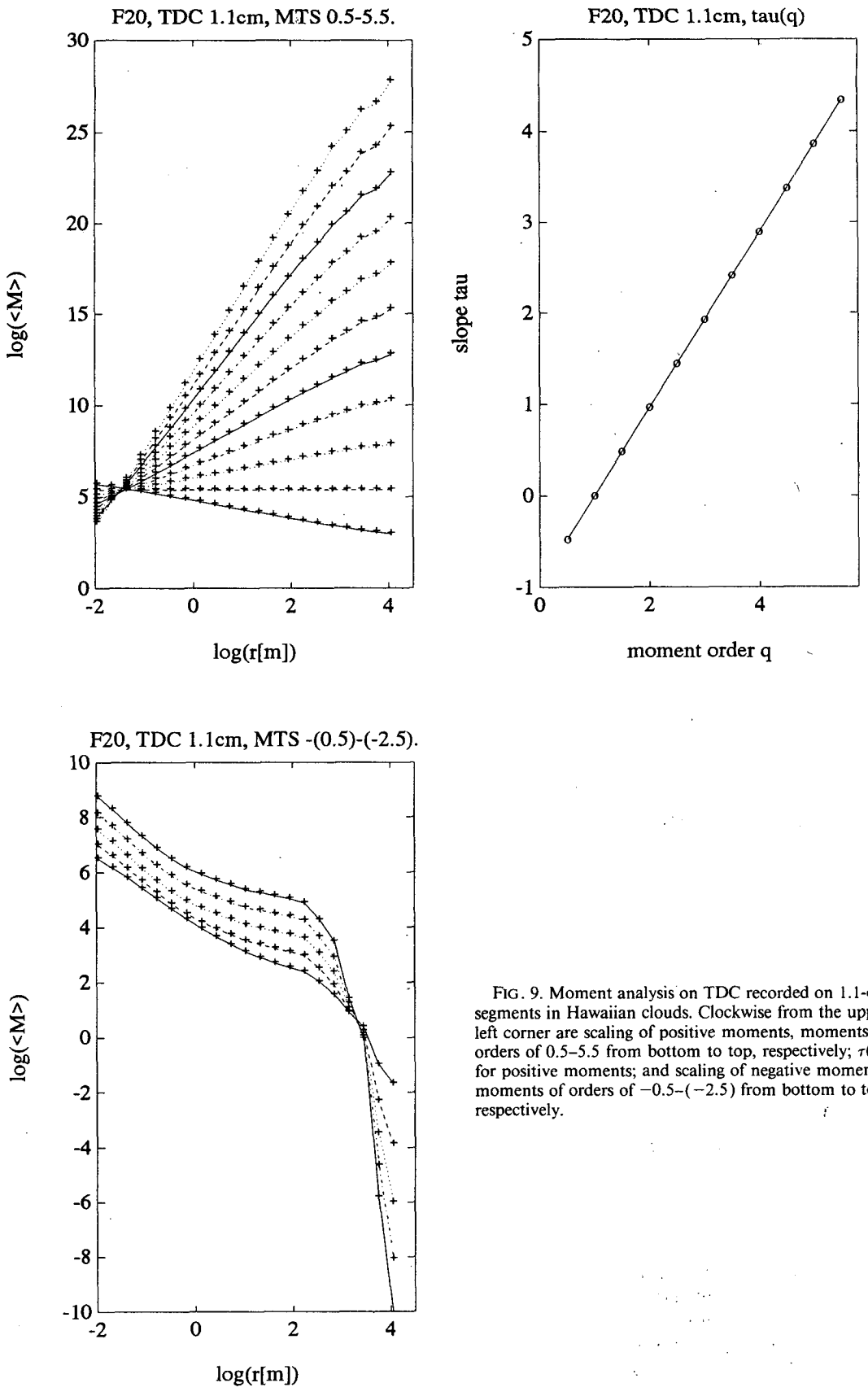

FIG. 9. Moment analysis on TDC recorded on 1.1-cm segments in Hawaiian clouds. Clockwise from the upper left corner are scaling of positive moments, moments of orders of 0.5–5.5 from bottom to top, respectively; $\tau(q)$ for positive moments; and scaling of negative moments, moments of orders of -0.5–(-2.5) from bottom to top, respectively.

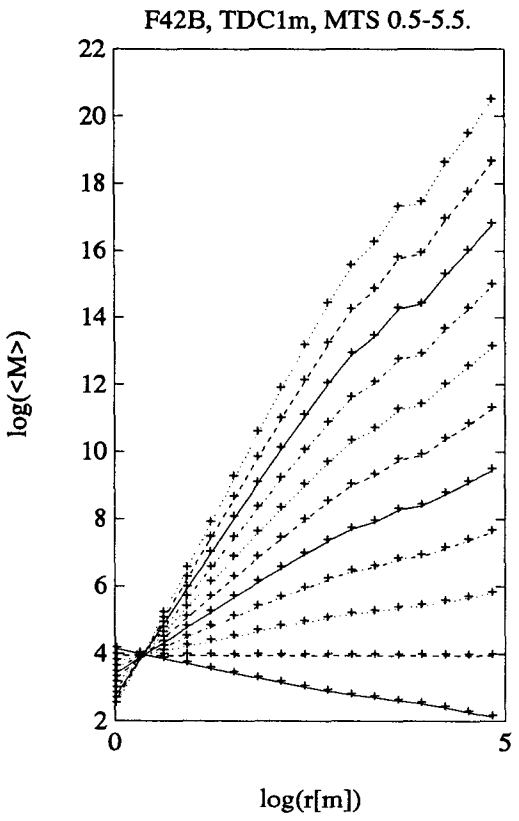

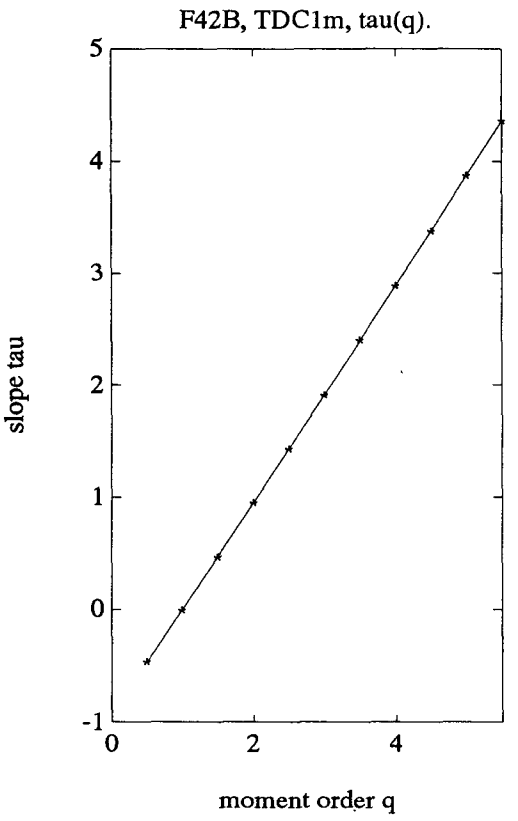

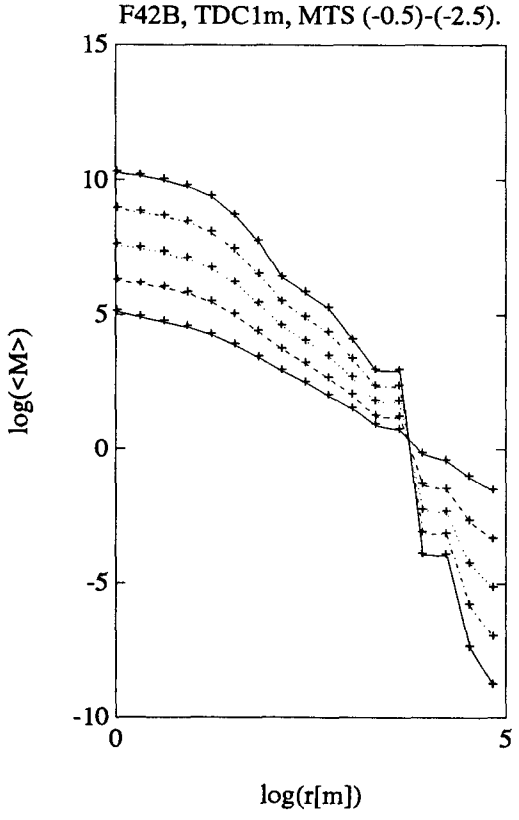

FIG. 10. Moment analysis on TDC recorded on 1 m segments in fair weather cumuli. Order of plots as in Fig. 9.

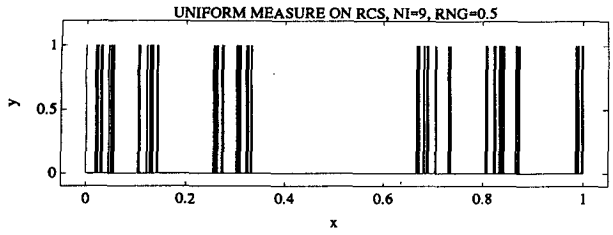

FIG. 11. Random Cantor set (RCS) with uniform measure. Realization for the random number seeder RNG = 0.5, 9 iterations.

leading to an increase in the estimated fractal dimension. According to the properties of the dimension, a set consisting of i subsets of dimensions D_i should have dimension D equal to the highest dimension of subsets: $D = \max(D_i)$. The above is valid for fractal sets with an infinite number of elements. For sets with a finite number of elements (as in our case) $\min(D_i) < D < \max(D_i)$ with a strong bias toward $\max(D_i)$, depending on the strength of the subsets. On the other hand, both fractal dimensions of the cloud–clear air interface and range of scales may depend not only on turbulence in clouds but also upon the turbulence in the cloud environment. Constantin et al. (1991) report that for passive scalar interfaces, the existence of external turbulence leads to an increase in the fractal dimension of an interface from 2.33 to 2.66. A similar increase can be true for clouds. In particular, cloud 6, a stratiform cloud formed in the dissipation stage of the rainband, can be influenced by the turbulent environment due to previous cloud activity. An increase in the fractal dimension of cloud–clear air interface in this case is not surprising. Raga et al. (1990), looking at entrainment into Hawaiian clouds with more traditional methods, point out various entrainment histories for various investigated cloud volumes. Our findings are in agreement with these observations. If clouds in various stages of their life cycle and with various fractal dimensions are included in the total dataset, the fractal dimension of this combined set should be close to the highest observed value in individual clouds. Thus, we can conclude that our results do not contradict the MZ findings. Malinowski and Zawadzki (1993) report that for fair weather cumuli, the fractal dimension is threshold independent over a wide range except close to the maximum. This indicates that TDC on a 1D section through such a cloud resembles the uniform measure on an RCS to Fig. 11 more closely than does TDC from Hawaiian clouds. This is presented in Fig. 15.

5. Summary and conclusions

1) No preferential clustering by droplet sizes is observed in 1D horizontal cross sections through clouds. In cloud volumes, droplets fill space in terms of fractal dimension for scales greater than 1 mm, suggesting that droplets are not distributed fractally inside cloud interiors.

2) Fractal analysis, analysis of distances between droplets, and the direct interpretation of high-resolution TDC data indicate that turbulent entrainment and mixing lead to cloud structure filamentation. Even in advanced stages of cloud dissipation, some filaments remain with local droplet concentrations similar to those in unmixed volumes. There are some indications of vertical anisotropy of these cloud remnants.

3) Cloud–clear air interface appears to be fractal in clouds in active development. In the stratiform part of the rainband as well as in the dissipating clouds, points delineating cloud–clear interface cannot be effectively retrieved by thresholding TDC records; thus, conclusions on the nature of this interface cannot be drawn. Fractal dimension $D_1 = 0.55$ observed by MZ in continental fair weather cumuli is confirmed for small thresholds only.

4) A uniform measure on RCS after a moderate number of iterations seems to have similar fractal properties as TDC records from FSSP probe.

Summarizing, we can say that in spite of state-of-the-art observations, much remains to be learned about the microstructure of clouds. This structure is extremely important in the estimation of the rate and effectiveness of cloud–environment mixing or evaporative cooling. Droplets evaporate or grow in response to conditions in their nearest vicinity, not to the average conditions. One-dimensional horizontal sections through clouds provide us with a lot of information; however, conclusions about the 3D structure of clouds cannot be drawn with certainty. It thus appears that undertaking studies on the 3D cloud structure at small scales by techniques such as holography (Conway et al. 1982; Kozikowska et al. 1984) are worthwhile. Significant information about the possible anisotropy in

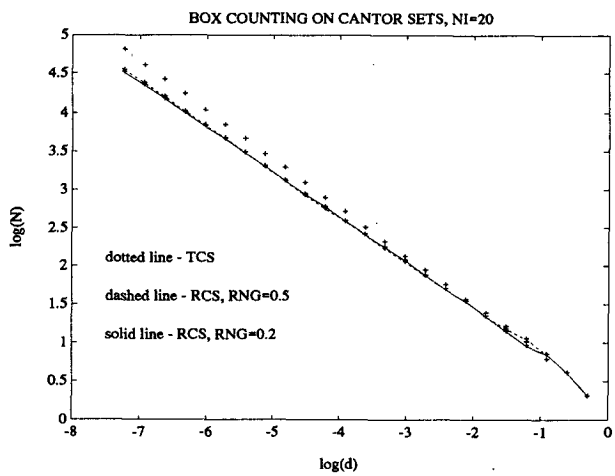

FIG. 12. Box counting on TCS and two different realizations of RCS (random number generator seeds 0.2. and 0.5) after 20 iterations.

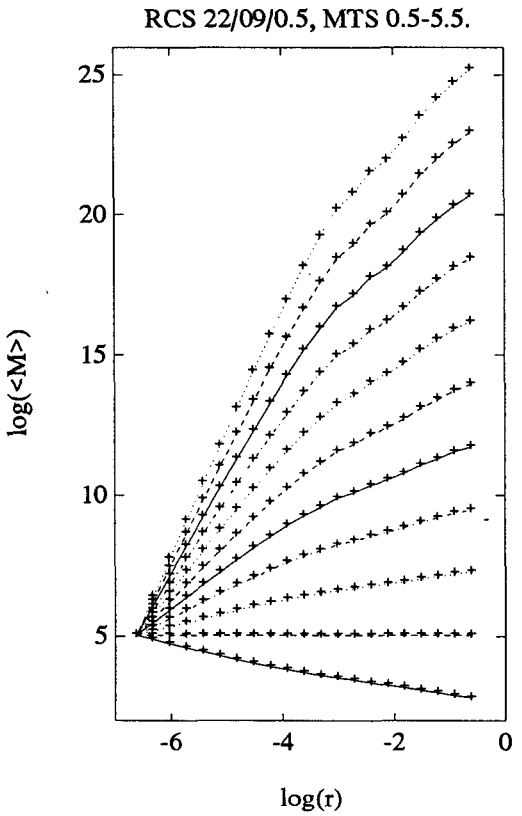

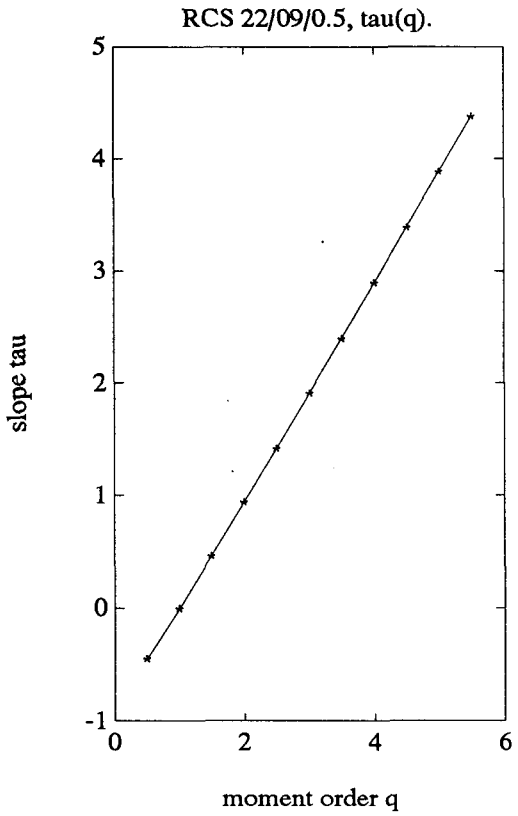

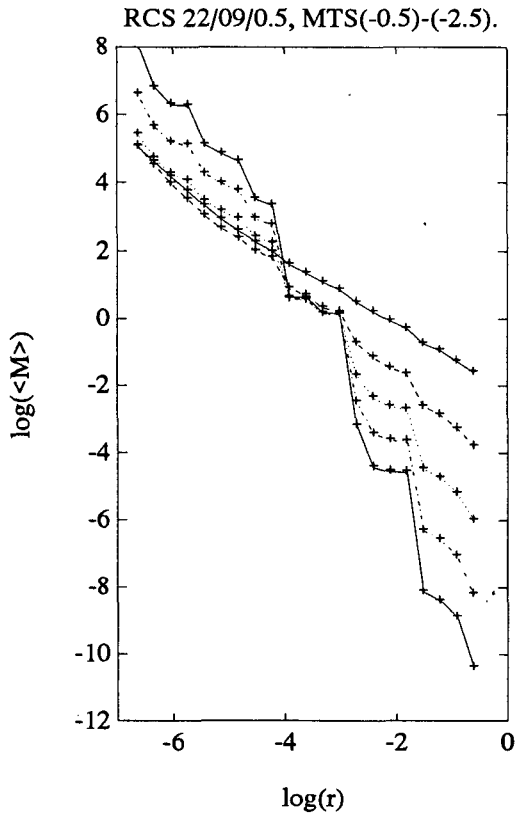

FIG. 13. Moment analysis of uniform measure on RCS after 9 iterations. Order of plots as in Fig. 9.

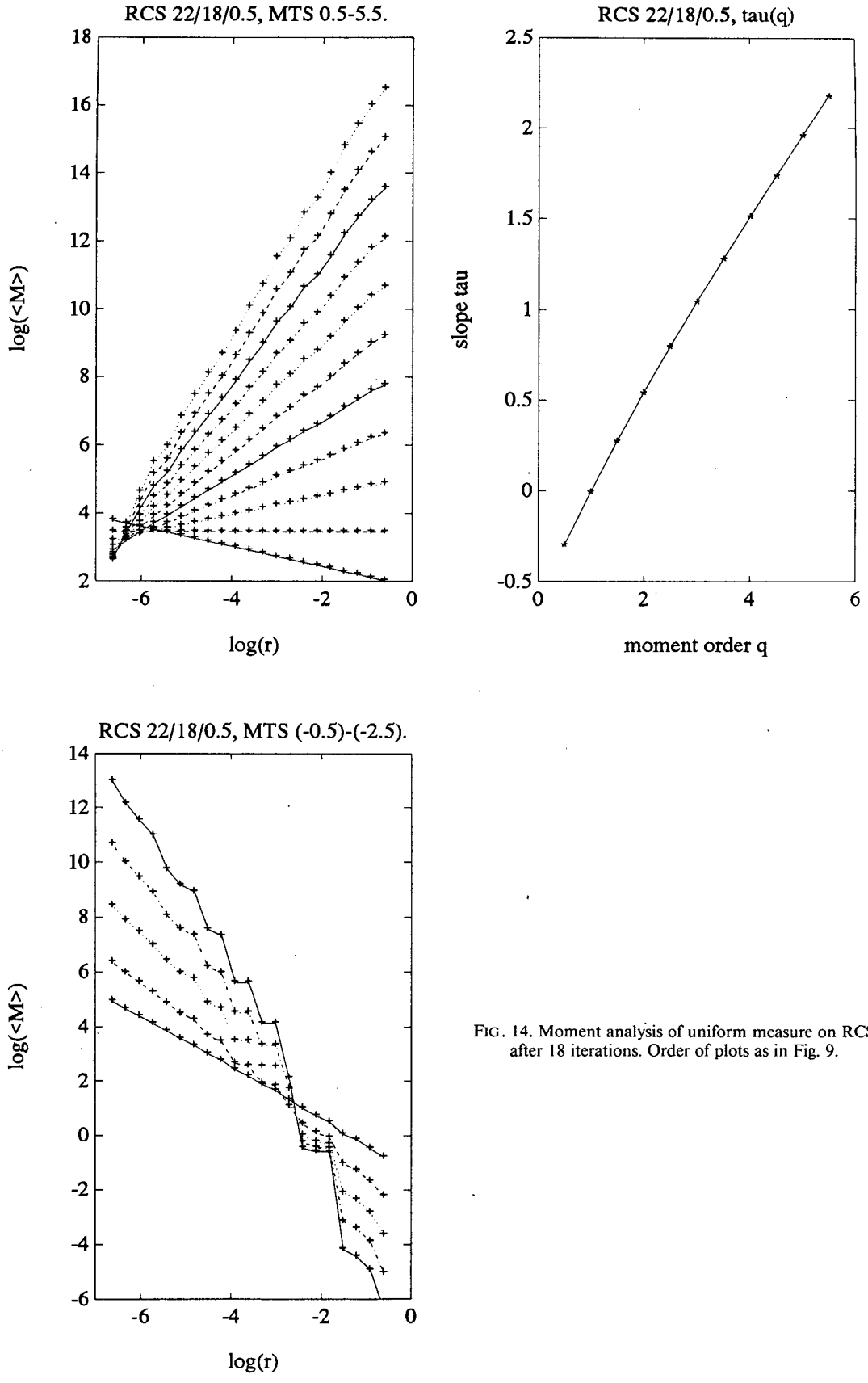

FIG. 14. Moment analysis of uniform measure on RCS after 18 iterations. Order of plots as in Fig. 9.

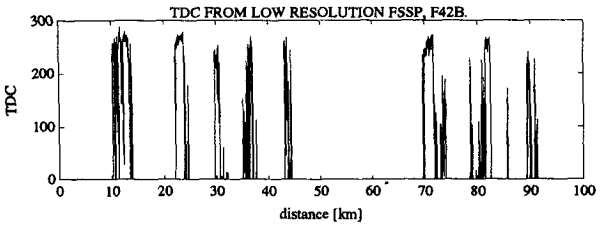

FIG. 15. TDC on 30-m segments collected in fair weather cumuli.

small-scale cloud structure could also be retrieved from vertical sections through clouds using high-resolution FSSP. More effort should be directed into high-resolution measurements of temperature, humidity, and velocity fields in cloud interiors in order to investigate the interaction between cloud microphysics and small-scale dynamics. Such a research program was already undertaken by the authors. Finally, we believe that experimental studies of intermittence and temporal evolution of turbulent energy field in clouds and their environment should result in a better understanding of the entrainment–mixing process.

Acknowledgments. The authors thank Dr. Wojciech Grabowski and Dr. Jean-Louis Brenguier for providing valuable remarks and suggestions. The authors are also indebted to anonymous reviewers for their thorough review and constructive comments. The paper was supported by the Fonds pour la Formation de Chercheurs et Aide la Recherche, the National Science and Engineering Research Council of Canada, and Atmospheric Environment Service. The National Center for Atmospheric Research is sponsored by the National Science Foundation.

REFERENCES

Baker, B. A., 1992a: Turbulent entrainment and mixing in clouds: A new observational approach. *J. Atmos. Sci.*, **49,** 387–404.

——, 1992b: "Inch clouds?" Observations of detrained and dissipating cloud. *Proc. 11th ICCP Conf.*, Montreal, IAMAP, International Association of Meteorology and Atmospheric Physics.

Baker, M. B., R. E. Breidenthal, T. W. Choularton, and J. Latham, 1984: The effects of turbulent mixing in clouds. *J. Atmos. Sci.*, **36,** 1612–1615.

Baumgardner, D., 1986: A new technique for the study of cloud microstructure. *J. Atmos. Oceanic Technol.*, **3,** 340–343.

——, B. Baker, and K. Weaver, 1993: A technique for the measurement of cloud structure on centimeter scales. *J. Atmos. Oceanic Technol.*, **10,** 557–565.

Brenguier, J-L., 1990: Parameterization of the condensation process in small nonprecipitating cumuli. *J. Atmos. Sci.*, **47,** 1127–1148.

——, and W. W. Grabowski, 1993: Cumulus entrainment and cloud droplet spectra. A numerical model within a two-dimensional dynamical framework. *J. Atmos. Sci.*, **50,** 120–136.

Broadwell, J. E., and R. E. Breidenthal, 1982: A simple model of mixing and chemical reaction in a turbulent shear layer. *J. Fluid. Mech.*, **125,** 397–410.

Cahalan, R. F., and J. H. Joseph, 1989: Fractal statistics of cloud fields. *Mon. Wea. Rev.*, **117,** 261–272.

Constantin, P., I. Procaccia, and K. R. Sreenivasan, 1991: Fractal geometry of isoscalar surfaces in turbulence: theory and experiments. *Phys. Rev. Lett.*, **67,** 1739–1742.

Conway, B. J., S. J. Caughley, A. N. Bentley, and J. D. Turton, 1982: Ground-based and airborne holography of ice and water clouds. *Atmos. Environ.*, **16,** 1193–1207.

Davis, A., S. Lovejoy, and D. Schertzer, 1991: Radiative transfer in multifractal clouds. *Scaling, Fractals and Nonlinear Variability in Geophysics,* D. Schertzer and S. Lovejoy, Eds., Kluwer, 303–318.

Falconer, K., 1990: *Fractal Geometry, Mathematical Foundations and Applications.* Wiley & Sons, 288 pp.

Feder, J., 1988: *Fractals.* Plenum Press, 283 pp.

Jensen, J. B., and M. B. Baker, 1989: A simple model of droplet spectral evolution during turbulent mixing. *J. Atmos. Sci.*, **46,** 2812–2829.

Kozikowska, A., K. Haman, and J. Supronowicz, 1984: Preliminary results of an investigation of the spatial distribution of fog droplets by a holographic method. *Quart. J. Roy. Meteor. Soc.*, **110,** 65–73.

Lovejoy, S., 1982: Area–perimeter relation for rain and cloud areas. *Science,* **216,** 185–187.

——, and D. Schertzer, 1990: Multifractal analysis techniques and the rain and cloud fields from 10^{-3} to 10^{6} m. *Scaling, Fractals and Nonlinear Variability in Geophysics.* D. Schertzer and S. Lovejoy, Eds. Kluwer, 318 pp.

MacPherson, J. I., and G. A. Isaac, 1977: Turbulent characteristics of some Canadian cumulus clouds. *J. Appl. Meteor.*, **16,** 81–90.

Malinowski, S. P., and H. Pawlowska-Mankiewicz, 1989: On estimating the entrainment level in cumulus clouds. *J. Atmos. Sci.*, **46,** 2463–2465.

——, and I. Zawadzki, 1993: On the surface of clouds. *J. Atmos. Sci.*, **50,** 5–13.

Mandelbrot, B. B., 1974: Intermittent turbulence in self-similar cascades: divergence of high moments and dimension of the carrier. *J. Fluid. Mech.*, **62**(Part 2), 331–358.

——, 1982: *The Fractal Geometry of Nature.* W. H. Freeman, 461 pp.

——, 1989: Multifractal measures, especially for the geophysicist. *Pure Appl. Geophys.*, **131,** 6–42.

Meneveau, C., and K. R. Sreenivasan, 1991: The multifractal nature of turbulent energy dissipation. *J. Fluid. Mech.*, **224,** 428–484.

Paluch, I. R., and D. G. Baumgardner, 1989: Entrainment and fine scale mixing in a continental convective cloud. *J. Atmos. Sci.*, **46,** 261–278.

Raga, G. B., J. B. Jensen, and M. B. Baker, 1990: Characteristics of cumulus band clouds off the coast of Hawaii. *J. Atmos. Sci.*, **47,** 338–355.

Sreenivasan, K. R., 1991: Fractals and multifractals in fluid turbulence. *Ann. Rev. Fluid Mech.*, **23,** 539–600.

——, R. Ramshankar, and C. Menevau, 1989: Mixing, entrainment and fractal dimensions of surfaces in turbulent flows. *Proc. R. Soc. London A,* **421,** 79–108.